JOURNAL
OF THE AMERICAN CHEMICAL SOCIETY

VOLUME 102, NUMBER 5 FEBRUARY 27, 1980

Aspects of Artificial Photosynthesis. Photosensitized Electron Transfer and Charge Separation in Cationic Surfactant Vesicles

Pierre P. Infelta, Michael Grätzel,* and Janos H. Fendler*[1]

Contribution from the Institut de Chimie Physique, Ecole Polytechnique Fédérale de Lausanne, Lausanne, Switzerland. *Received July 5, 1979*

Abstract: Electron transfer and charge separation have been investigated in cationic dioctadecyldimethylammonium chloride (DODAC) vesicles by laser spectroscopy. *N*-Methylphenothiazine (MPTH) and its long-chain analogue, *N*-dodecylphenothiazine (DPTH), were used as electron donors, while a surfactant derivative of tris(2,2′-bipyridine)ruthenium perchlorate, $RuC_{18}(bpy)_3^{2+}$, acted as the photoactive electron acceptor. DODAC vesicles organized these donor and acceptor molecules. $RuC_{18}(bpy)_3^{2+}$ molecules were anchored onto the surface of the vesicles, while MPTH molecules were distributed among the hydrophobic bilayers of the vesicles. The metal to ligand charge transfer excited state of the ruthenium complex, $RuC_{18}(bpy)_3^{2+*}$, readily accepted an electron from MPTH to give $MPTH^{+\cdot}$ and $RuC_{18}(bpy)_3^{+}$. Three different pathways have been recognized for the reaction of $MPTH^{+\cdot}$ with $RuC_{18}(bpy)_3^{+}$. First, there is a rapid geminate recombination at the very site of the generation of the cation radical. Second, some of the $MPTH^{+\cdot}$ escapes into the vesicle entrapped water pools and, owing to spatial confinement, the combination occurs at the inner surface of the vesicles. Finally, a part of $MPTH^{+\cdot}$ escapes into the bulk aqueous solution where it survives for extended periods ($\gg$1 ms). Effects of MPTH and NaCl concentrations on these pathways have been examined. Both affect the outer surface charge density of the vesicles. In addition, the chloride ions modify the net charge and the potential gradient across the vesicle bilayers. Changes in lifetimes and yields in the charge-separated products are brought about. The amounts of $MPTH^{+\cdot}$ produced and that expelled into the bulk aqueous solution were maximized in the presence of 1.0×10^{-3} M NaCl. Under this condition there was still a sufficient electrostatic repulsion between $MPTH^{+\cdot}$ and the charged surface of the vesicles to slow down considerably the undesirable charge recombination reactions. Carrying out the electron transfer using DPTH resulted only in short-lived $DPTH^{+\cdot}$ in low concentrations. The long hydrocarbon chain on this molecule prevented the expulsion of this cation radical from the vesicle. Relevance of this study to light-induced photochemical energy conversion is discussed.

Introduction

Separation of charges, formed in photoinduced redox processes, is an essential requirement for efficient solar energy conversion.[2,3] Polyelectrolytes,[4-7] monolayers,[8-11] micelles,[2,12-20] and liposomes[21-24] have been utilized to facilitate charge separation. These systems organize donors and acceptors, lower ionization potentials, and, most importantly, through their interfaces or electrical double layers, allow for some kinetic control of electron transfers.

Surfactant vesicles offer potentially alternative attractive media for a selective organization of electron donor–acceptor couples. Significantly, unlike micelles,[25] they are static entities and able to accommodate a substantial number of guest molecules per aggregate. Vesicles readily form upon the ultrasonic dispersal of relatively simple cationic and anionic long-chain dialkyl surfactants.[26-32] They possess most of the desirable characteristics of liposomes[33,34] but they are chemically stable and easy to prepare and functionalize.[31,32] Pyrene, entrapped in completely synthetic dihexadecyl phosphate (DHP) vesicles, photoionizes.[35] The polarity gradient drives the electron into the aqueous phase and the back reaction with pyrene cation radicals is precluded by the net negative charge on the DHP vesicles.

Advantage is taken of positively charged dioctadecyldimethylammonium chloride (DODAC) vesicles in the present work. DODAC vesicles are stable for weeks in the pH 2–12 range, have phase transition temperatures at 30.0 and 36.2 °C, and are osmotically active and able to entrap polar and apolar molecules.[27-32] We report here the electron transfer to photoexcited tris(2,2′-bipyridine)ruthenium^{2+}, anchored onto the surface of DODAC vesicles by a long hydrocarbon chain, from *N*-methylphenothiazine (MPTH) distributed in the hydrophobic bilayers of DODAC vesicles. The MPTH cation radicals formed are expelled both into the vesicle entrapped and into bulk water. The amounts of $MPTH^{+\cdot}$ formed and the extent and rate of subsequent charge recombinations are functions of the concentrations of MPTH in the vesicles as well as added sodium chloride. Using dodecylphenothiazine (DPTH) instead of MPTH resulted in the formation of negligible amounts of cation radicals and in fast subsequent charge recombination.

Experimental Section

Syntheses, purifications, and characterizations of dioctadecyldimethylammonium chloride (DODAC)[31,32] and *N*-methylphenothiazine (MPTH)[19] have been previously described. *N*-Dodecyl-

0002-7863/80/1502-1479$01.00/0

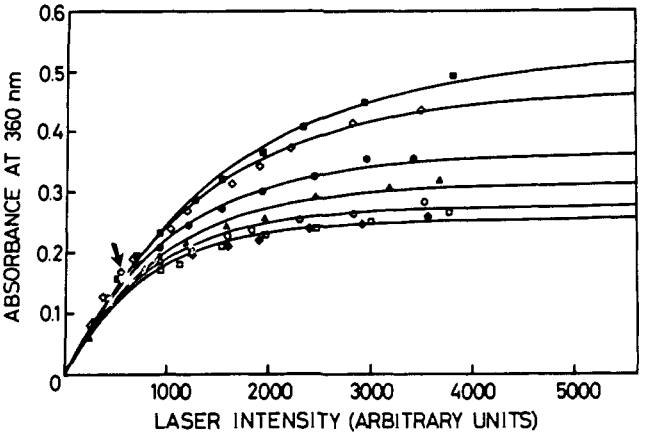

Figure 1. Absorbances of $RuC_{18}(bpy)_3^{2+}$* as functions of laser intensity in 2.55×10^{-3} M DODAC intercalated 8.9×10^{-5} M $RuC_{18}(bpy)_3^{2+}$ in the presence of 0 (■), 5.0×10^{-4} (◇), 1.0×10^{-3} (●), 2.0×10^{-3} (▲), 4.0×10^{-3} (○), 8.0×10^{-3} (□), and 1.6×10^{-2} M (♦) NaCl. Arrow indicates the laser intensities used in electron-transfer experiments.

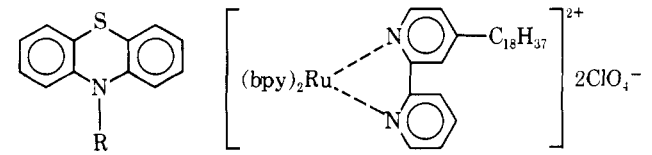

MPTH, R = CH_3
DPTH, R = $C_{12}H_{25}$

$RuC_{18}(bpy)_3^{2+}$

phenothiazine (DPTH) was donated by Dr. Andre Braun of this institution and long-chain tris(2,2′-bipyridine)ruthenium perchlorate, $RuC_{18}(bpy)_3^{2+}$, was donated by Dr. Wolfgang H. F. Sasse of the Division of Applied Organic Chemistry, CIRO, Australia. All other chemicals were the best available reagent grade.

DODAC vesicles were prepared by the ultrasonic dispersal of 36 mg of surfactant in 6.0 mL of triply distilled water, thermostated at 55 °C. Sonication was carried out by means of a Branson B-12 sonifier at 70 W for 3 min. Substrates were incorporated into the vesicles by sonicating appropriate amounts of MPTH, DPTH, or $RuC_{18}(bpy)_3^{2+}$, deposited in the form of thin films on vials by evaporating the solvent from alcoholic stock solutions, with diluted DODAC vesicles. These sonications were also carried out to 70 W for 4–6 min at 55 °C. DODAC solutions of MPTH and $RuC_{18}(bpy)_3^{2+}$ or DPTH and $RuC_{18}(bpy)_3^{2+}$ were optically transparent and remained stable for weeks. Solutions were degassed by bubbling with 99.999% pure argon passed through Oxisorb to remove any trace of oxygen.

Steady-state absorption and emission spectra were taken on a Varian Cary 219 spectrophotometer and a Perkin-Elmer MPF-44 spectrofluorometer, respectively. The frequency doubled pulsed neodymium laser (JK-2000, 530 nm, 15 ns) and associated detection system have been previously described.[36]

Results and Discussion

Steady-State Spectra. The absorption spectrum of $RuC_{18}(bpy)_3^{2+}$, both in alcohol and in DODAC vesicles, is entirely analogous to that reported for tris(2,2′-bipyridine)-ruthenium chloride.[37] Thus, vesicle intercalated $RuC_{18}(bpy)_3^{2+}$, containing 2.55×10^{-3} M stoichiometric DODAC, shows two absorption maxima with ϵ_{452nm} 1.6×10^4 M^{-1} cm^{-1} and ϵ_{287nm} 8.7×10^4 M^{-1} cm^{-1}. Absorption spectrum of MPTH or DPTH in DODAC vesicles (2.55×10^{-3} M stoichiometric DODAC) shows only an ultraviolet peak, ϵ_{310nm} 5.4×10^3 M^{-1} cm^{-1}. The presence of MPTH or DPTH does not alter, therefore, the absorption due to $RuC_{18}(bpy)_3^{2+}$ at 452 nm. Addition of NaCl, in the $(5-320) \times 10^{-4}$ M region, increases the turbidity of DODAC vesicles, but only alters the absorption at 452 nm by 3% at the most. Absorption spectra of each solution were shown to be identical prior and subsequent to each set of laser photolysis experiments. Excitation of $RuC_{18}(bpy)_3^{2+}$ in DODAC vesicles, both at 460 and 530 nm, resulted in a luminescence spectrum with an emission maximum at 620 nm. The emission maximum of $[Ru(bpy)_3^{2+}]2Cl^-$ was reported to vary from 605 nm in water to 625 nm in aqueous micellar sodium dodecyl sulfate.[6] Apparently, the chromophore of $RuC_{18}(bpy)_3^{2+}$ is in a relatively hydrophobic environment in DODAC vesicles. Addition of MPTH quenches the luminescence intensity of $RuC_{18}(bpy)_3^{2+}$. Emission intensity is also slightly quenched (<3%) by NaCl.

Laser Photolysis of DODAC Vesicle Intercalated Long Chain Tris(2,2′-bipyridine)ruthenium Perchlorate, $RuC_{18}(bpy)_3^{2+}$. Laser excitation of DODAC intercalated $RuC_{18}(bpy)_3^{2+}$ resulted in the appearance of a transient absorption, with a maximum at 370 nm, in the bleaching of the ground-state absorption, at 450 nm, and in a long-lived luminescence, with an emission maximum at 620 nm. The transient absorbing at 370 nm is due to the metal to ligand charge transfer excited state of the ruthenium complex, $RuC_{18}(bpy)_3^{2+}$*. The amounts of $RuC_{18}(bpy)_3^{2+}$* formed, at a given laser intensity, depended somewhat on the concentration of $RuC_{18}(bpy)_3^{2+}$ intercalated in the DODAC vesicles. Stoichiometric 8.9×10^{-5} M $RuC_{18}(bpy)_3^{2+}$ appeared to be the optimum concentration. This concentration of $RuC_{18}(bpy)_3^{2+}$ was used, therefore, in all subsequent work.

Initial experiments were performed to explore the effect of the energy content of the laser on the concentration of $RuC_{18}(bpy)_3^{2+}$* formed as a function of added NaCl.[38] Figure 1 shows changes of optical densities of $RuC_{18}(bpy)_3^{2+}$* at the beginning of the laser pulse, in the absence and in the presence of different amounts of added NaCl. The observed effect seems to be due to a variation in the light-scattering properties of the vesicles. As the energy content of the laser pulse was measured, the fraction of it absorbed by $RuC_{18}(bpy)_3^{2+}$ varied. Therefore, all experiments were carried out at relative laser intensities of 700 or less (on the arbitrary scale given in Figure 1). This corresponded to ~50 mJ/pulse.

Laser Photolysis of DODAC Vesicle Intercalated Long Chain Tris(2,2′-bipyridine)ruthenium Perchlorate, $RuC_{18}(bpy)_3^{2+}$, and MPTH. All experiments were carried out at constant stoichiometric concentrations of DODAC = 2.55×10^{-3} M and $RuC_{18}(bpy)_3^{2+}$ = 8.9×10^{-5} M. The concentration of MPTH was varied between 2.38×10^{-6} and 1.19×10^{-3} M. Transient absorbances with maxima at 370 and 510 nm were detected with concomitant bleaching of the ground-state absorbance of $RuC_{18}(bpy)_3^{2+}$ at 450 nm. On the microsecond time scale, the bleaching recovered at the expense of the absorbance at 370 nm. The absorbance at 510 nm did not, however, disappear even 500 μs after the pulse. The transient absorbance at 370 nm originates in $RuC_{18}(bpy)_3^{2+}$*, and that at 510 nm is a composite of the absorption due to $MPTH^{+}\cdot$ (ϵ_{510} 9.3×10^3 M^{-1} cm^{-1}) and $RuC_{18}(bpy)_3^{+}\cdot$ (ϵ_{510} 1.9×10^4 M^{-1} cm^{-1}).[39]

Detection of $MPTH^{+}\cdot$ is a function of MPTH concentration in the DODAC vesicles. At 2.3×10^{-6} M stoichiometric MPTH concentration, no $MPTH^{+}\cdot$ could be detected at any laser energies (up to 200 mJ). In the $(8-24) \times 10^{-6}$ M stoichiometric MPTH range only meager amounts of $MPTH^{+}\cdot$ are detectable (absorbances at 510 nm are in the range of 0.005–0.002). At higher MPTH concentrations $MPTH^{+}\cdot$ becomes easily detectable (vide supra). Detection of $MPTH^{+}\cdot$ is also a function of the temperature. Transient absorbances at 510 nm, particularly those formed at lower stoichiometric MPTH concentrations, decrease markedly if the temperature is increased to 38 °C or higher. This effect is due to the thermotropic phase transition of DODAC vesicles at 37 °C.[31,32] At the phase transition temperature, vesicles become fluid, which results, presumably, in decreased electron transfer from MPTH to $RuC_{18}(bpy)_3^{2+}$* and in increased charge recombinations. Original absorbances of $MPTH^{+}\cdot$ were recovered

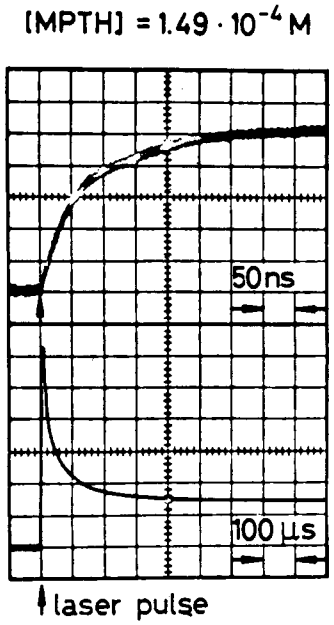

Figure 2. Time dependence of the transient absorbance at 510 nm in 2.55 × 10^{-3} M DODAC intercalated 8.9 × 10^{-5} M $RuC_{18}(bpy)_3^{2+}$ in the presence of 1.49 × 10^{-4} M MPTH.

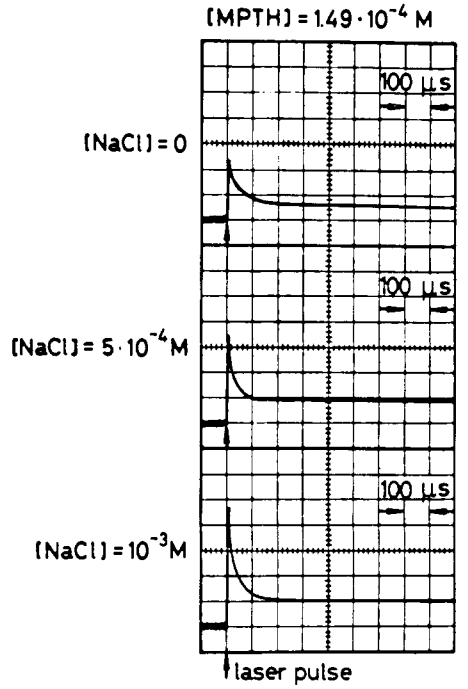

Figure 3. Transient absorbance changes at 510 nm in 2.55 × 10^{-3} M DODAC intercalated 8.9 × 10^{-5} M $RuC_{18}(bpy)_3^{2+}$ in the presence of the indicated amounts of MPTH and NaCl. (The vertical scale is identical for all traces.)

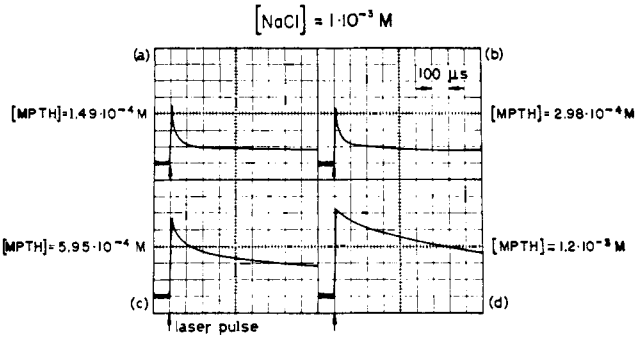

Figure 4. Transient absorbance changes at 510 nm in 2.55 × 10^{-3} M DODAC intercalated 8.9 × 10^{-5} M $RuC_{18}(bpy)_3^{2+}$ in the presence of the indicated amounts of MPTH and NaCl. (The vertical scale is identical for all traces.)

on cooling the solutions to ambient temperature.

Rate constants for the recovery of the bleaching of the absorbance at 450 nm, for the decay of $RuC_{18}(bpy)_3^{2+}$* at 360 nm, and for the decrease of the luminescence intensity at 620 nm are identical in each solution. A typical time dependence of the transient absorbance at 510 nm is illustrated in Figure 2. The absorbance at 510 nm is seen to build up rapidly (the rate constant for this process is 6.0 × 10^6 s^{-1}) and decay slowly in a multistep process; substantial parts of it remain even milliseconds after the laser pulse.[40]

Subsequent to the formation of the metal to ligand charge transfer excited ruthenium complex

$$RuC_{18}(bpy)_3^{2+} \xrightarrow{h\nu} RuC_{18}(bpy)_3^{2+*} \quad (1)$$

a number of reaction pathways are possible. $RuC_{18}(bpy)_3^{2+*}$ may decay to the ground state by luminescence and radiationless transition:

$$RuC_{18}(bpy)_3^{2+*} \rightarrow RuC_{18}(bpy)_3^{2+} \quad (2)$$

It can capture an electron from a neighboring MPTH molecule:

$$RuC_{18}(bpy)_3^{2+*} + MPTH \rightarrow RuC_{18}(bpy)_3^{+} + MPTH^{+}\cdot \quad (3)$$

The $MPTH^{+}\cdot$ formed can disappear by a geminate-type[41] back electron transfer:

$$RuC_{18}(bpy)_3^{+}\cdot + MPTH^{+}\cdot \xrightarrow{\text{geminate}} RuC_{18}(bpy)_3^{2+} + MPTH \quad (4)$$

The appearance of the transient absorbances at 510 nm is the result of the formation of the two radical cations (reaction 3) and their concomitant disappearance via geminate recombinations (reaction 4).

Understanding of the electron transfer and the subsequent fate of $MPTH^{+}\cdot$ has required an examination of the effects of added NaCl and altered MPTH concentrations. Figure 3 shows the influence of NaCl on $MPTH^{+}\cdot$ absorbances observed in DODAC vesicles containing $RuC_{18}(bpy)_3^{2+}$ and MPTH. Both the prompt and the long-term yields of $MPTH^{+}\cdot$ are seen to increase with increasing concentrations of NaCl. There is only a slight increase of the long-term yield. Effects of MPTH concentrations, at a given NaCl concentration, are illustrated in Figure 4. Both the prompt and the long-time yields of $MPTH^{+}\cdot$ are seen to increase with increasing concentrations of MPTH, at the particular concentrations of NaCl illustrated. The kinetic behavior of the decay should also be pointed out. At low MPTH concentrations a substantial fraction of $MPTH^{+}\cdot$ decays within 100 µs. As the MPTH concentration is increased the longer lived fraction of $MPTH^{+}\cdot$ becomes more predominant. At the highest MPTH concentration, there is only an apparent one-step process at the time scale investigated.

Table I allows a somewhat more general discussion of the results. In the absence of NaCl, the general trend shows an increase in the half-life time and the absorbance of $MPTH^{+}\cdot$ with increasing MPTH. A detailed inspection of the data reveals, however, a more subtle behavior. This can be rationalized by considering the nature of the present system. The $MPTH^{+}\cdot$, formed in reaction 3, can promptly back-react at the very site of its generation (reaction 4). Additionally, potential gradients, provided by the surface charge densities of the vesicles, pro-

Table I. Absorbances and Half-Life Times of $MPTH^{+}\cdot$ in 2.55×10^{-3} M DODAC Intercalated 8.9×10^{-5} M $RuC_{18}(bpy)_3^{2+}$ as a Function of MPTH Concentration in the Absence and in the Presence of 1.0×10^{-3} M NaCl

	[NaCl] = 0			[NaCl] = 1.0×10^{-3} M		
10^4 [MPTH], M	$10^6 t_{1/2}$, s	absorbance max, 510 nm	absorbance at 500 μs, 510 nm	$10^6 t_{1/2}$, s	absorbance max, 510 nm	absorbance at 500 μs, 510 nm
1.49	20.0	0.0236	0.0048	20.0	0.0362	0.0074
2.98	2.0	0.0253	0.0041	16.0	0.0485	0.0083
5.95	100.0	0.0290	0.0096	180.0	0.0470	0.0200
11.90	1000.0	0.0342	0.0221	730.0	0.0504	0.0297

mote the exit of $MPTH^{+}\cdot$. $MPTH^{+}\cdot$ can exit either into the DODAC-entrapped water pools or into the bulk solution. Subsequent diffusion of the cation radical results in a combination with $RuC_{18}(bpy)_3^{+}\cdot$ either at the inner (reaction 4′) or at the outer (reaction 4″) surface of the vesicles.

$$RuC_{18}(bpy)_3^{+}\cdot + MPTH^{+}\cdot \xrightarrow{\text{inner surface}} RuC_{18}(bpy)_3^{2+} + MPTH \quad (4')$$

$$RuC_{18}(bpy)_3^{+}\cdot + MPTH^{+}\cdot \xrightarrow{\text{outer surface}} RuC_{18}(bpy)_3^{2+} + MPTH \quad (4'')$$

The spatial confinement of some of the $MPTH^{+}\cdot$ in the vesicle-entrapped water pools renders reaction 4′ faster than reaction 4″. This is substantiated by the observed kinetic behavior of the decay of $MPTH^{+}\cdot$ (see Figures 3 and 4). The faster component of this decay is attributed to (4′) and the long-lived component to (4″). The decrease of the half-life time of $MPTH^{+}\cdot$ in going from 1.49×10^{-4} to 2.98×10^{-4} M MPTH concentration (Table I) is a consequence of an apparent favoring of the partitioning into the vesicle-entrapped water pools. Further addition of MPTH results in the formation of higher concentrations of the cation radical. This leads to an increased concentration of $MPTH^{+}\cdot$ in the vesicle-entrapped water pools to such an extent that a potential gradient is created. Any additional $MPTH^{+}\cdot$ formed is, therefore, driven into the bulk solution. Increasing the MPTH concentration results in more efficient quenching of the excited state and also in a decrease of the charge density on DODAC vesicles ([DODAC]:[MPTH] = 2.1 at the highest [MPTH]!) which favors the exit of $MPTH^{+}\cdot$. This is manifested in increased amounts of absorbances (see Table I).

Addition of NaCl provides a greater control of the processes described by reactions 3, 4, 4′, and 4″. In the range of concentrations used, NaCl does not penetrate the DODAC vesicles.[32] Added chloride ions decrease the fractional positive charges on the outer surface of DODAC vesicles. This has three important consequences. First, the number of sites, where the local electrostatic field prevented the existence of $MPTH^{+}\cdot$, is reduced. Second, a dissymmetry is created between the inner and outer surface potential of the vesicles which will increase the fraction of $MPTH^{+}\cdot$ exiting into the bulk solution. Third, the reduced net charge on the aggregates increases the rate of reaction 4″.

Addition of NaCl, up to 2.0×10^{-3} M concentration, drastically increases the prompt amount of $MPTH^{+}\cdot$ formed (see upper portion of Figure 5). Apparently, when the NaCl concentration reaches that of the DODAC, most of the positive charge on the outer surface of vesicles is neutralized. Further addition of electrolytes can no longer influence the local electrostatic field. Increased fractions of the long-lived component of $MPTH^{+}\cdot$ with increasing NaCl concentrations (see Figure 4 and compare the upper and lower portions of Figure 5) are manifestations of the dissymmetry in the electrostatic field between the inner and the outer surface of the vesicles. While no further increase in the prompt amounts of $MPTH^{+}\cdot$ formed can be obtained on addition of NaCl beyond 2.0×10^{-3} M (see the upper portion of Figure 5), the reduction of the net surface charge on the aggregates causes a drastic loss of the long-lived species (see the lower portion of Figure 5) via acceleration of reaction 4″. Table I details the most pronounced case, the effect of 1.0×10^{-3} M NaCl on the amounts of $MPTH^{+}\cdot$ and on the half-life time of its decay.

From the foregoing considerations, we present Figure 6 as a plausible model for light-induced electron transfer and subsequent charge separations in DODAC vesicles.

Laser Photolysis of DODAC Vesicle Intercalated Long Chain Tris(2,2′-bipyridine)ruthenium Perchlorate, $RuC_{18}(bpy)_3^{2+}$, and Dodecylphenothiazine, DPTH. Laser photolysis of vesicle intercalated $RuC_{18}(bpy)_3^{2+}$ and DPTH resulted in the bleaching of the ground-state absorption, at 450 nm, and the parallel appearance of $RuC_{18}(bpy)_3^{2+*}$ absorbance at 360 nm. Rate constants for the bleaching agreed with that for the decay of $RuC_{18}(bpy)_3^{2+*}$ absorbance and were on the order of $(2\text{-}3) \times 10^6$ M^{-1} s^{-1}. This behavior is quite analogous to that observed for DODAC-entrapped $RuC_{18}(bpy)_3^{2+}$ and MPTH.

There is a significant difference, however, between $MPTH^{+}\cdot$ and its long-chain analogue, $DPTH^{+}\cdot$. In the absence of sodium chloride, an absorbance of only 0.008 could be detected at 510 nm in DODAC-entrapped 8.9×10^{-5} M $RuC_{18}(bpy)_3^{2+}$ and 2.9×10^{-4} M DPTH. The transient absorbance at 510 nm at comparable concentrations of MPTH was 0.03. Even more significantly, $DPTH^{+}\cdot$ decayed completely in a relatively short time (ca. 6 μs).

Conclusion

Completely synthetic surfactant vesicles have been exploited in the present work for mimicking the photosynthetic apparatus. Photoinduced electron transport and charge separation have been accomplished in a deceptively simple system containing a cationic surfactant, an electron donor, and an electron acceptor.

Organization of suitable molecules is provided by the different compartments available in surfactant vesicles. Thus, polar uncharged species can be entrapped into the aqueous inner compartments of the vesicles or remain outside in the bulk solution. Charged species can be attracted to their gegenions, located at the inner and at the outer surface of the aggregates. Species having charges identical with that on the vesicles can be anchored by suitable hydrocarbon chains. Incorporation of $RuC_{18}(bpy)_3^{2+}$ into cationic DODAC vesicles, described in the present work, illustrates this mode of interaction. Apolar probes are distributed in the bilayers of the vesicles. The extent of their mobilities depends, among other things, on their sizes and geometries. Thus, the relatively small MPTH molecule is fairly mobile. Subsequent to electron transfer, a fraction of the $MPTH^{+}\cdot$ formed was shown to be readily expelled into the aqueous inner compartments of the vesicles and into the bulk solution. In this latter environment, $MPTH^{+}\cdot$ lived so long that we could not detect its decay under our conditions(i.e., $t_{1/2} \gg 1$ ms). Conversely, the long hydrocarbon chain on DPTH precludes the analogous exit of

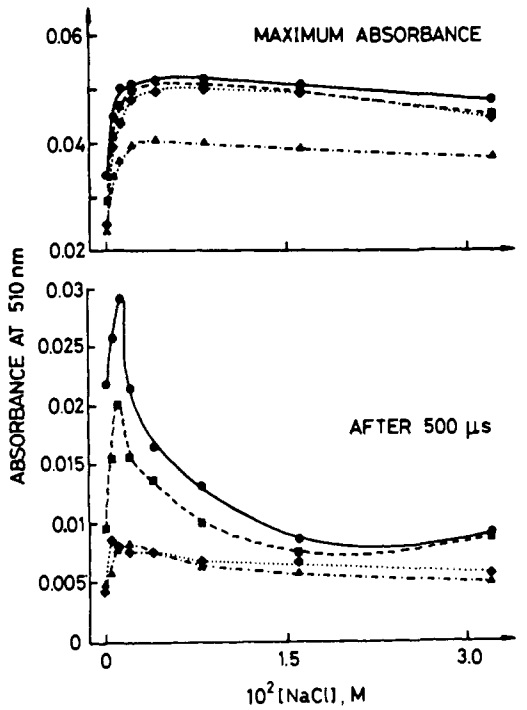

Figure 5. Absorbances due to $MPTH^{+\cdot}$ 1 (maximum absorbance) and 500 μs after laser pulse as function of added NaCl in 2.55×10^{-3} M DODAC intercalated 8.9×10^{-5} M $RuC_{18}(bpy)_3^{2+}$ containing 1.49×10^{-4} (▲), 2.98×10^{-4} (♦), 5.95×10^{-4} (■), and 1.2×10^{-3} M MPTH.

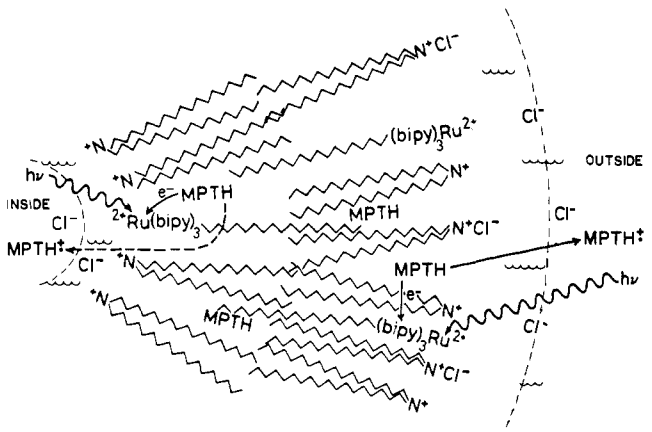

Figure 6. A schematic representation of DODAC vesicle intercalated $RuC_{18}(bpy)_3^{2+}$ and MPTH photoinduced electron transfer system.

$DPTH^{+\cdot}$ in appreciable amounts. The relative ease of synthetic modification of vesicle-forming surfactants may allow an even greater diversity in the potential organization of appropriate redox systems.

Important features of synthetic surfactant vesicles are their high surface potential and charge densities. These can provide a driving force for charge separation and diminish back-reactions. Judicious manipulations of added electrolytes have resulted in altered electrostatic fields at the outer surface of the vesicles. This dissymmetry can, in turn, allow for some control of the partitioning of the exiting charged species between the inner aqueous compartment of the vesicles and the bulk solution. Care must be exercised, however, not to neutralize the charges on the outer surface of the surfactant vesicles to an extent greater than needed for the electrostatic repulsion to prevent charge recombinations.

The present work has laid the foundations of more complex systems capable of separating oxidation and reduction units. Currently we are applying the principles learned in this and previous work[29-32] to the design of improved models containing chlorophyll and colloidal redox catalyzers as their components.

Acknowledgments. Support of this work in Lausanne by the Swiss National Research Fund, Grant 4.071,076.04, and in Texas by the National Science Foundation and the Robert A. Welch Foundation is gratefully acknowledged. The authors appreciate the generous donations of Dr. Andre Braun of EPFL and Dr. Wolfgang H. F. Sasse of the Division of Applied Organic Chemistry, CIRO, Australia, of samples.

References and Notes

(1) On leave from the Department of Chemistry, Texas A&M University, College Station, Texas 77843.
(2) M. Grätzel in "Micellization, Solubilization and Microemulsions", K. L. Mittal, Ed., Plenum Press, New York, 1977, p 531; M. Calvin, *Acc. Chem. Res.*, **10**, 369 (1978).
(3) G. Porter and M. V. Archer, *Interdiscip. Sci. Rev.*, **1**, 119 (1976).
(4) D. Meisel and M. Matheson, *J. Am. Chem. Soc.*, **99**, 6577 (1977).
(5) D. Meisel, J. Rabani, D. Meyerstein, and M. Matheson, *J. Phys. Chem.*, **82**, 985 (1978).
(6) D. Meisel, M. S. Matheson, and J. Rabani, *J. Am. Chem. Soc.*, **100**, 117 (1978).
(7) D. Meyerstein, J. Rabani, M. S. Matheson, and D. Meisel, *J. Phys. Chem.*, **82**, 1879 (1978).
(8) S. J. Valenty and G. L. Gaines, Jr., *J. Am. Chem. Soc.*, **99**, 1285 (1977).
(9) G. Sprintschnik, H. W. Sprintschnik, P. P. Kirsch, and D. G. Whitten, *J. Am. Chem. Soc.*, **99**, 4947 (1977).
(10) G. L. Gaines, Jr., P. E. Behnken, and S. J. Valenty, *J. Am. Chem. Soc.*, **100**, 6549 (1978).
(11) K.-P. Seefeld, D. Möbius, and H. Kuhn, *Helv. Chim. Acta*, **60**, 2608 (1977).
(12) M. Grätzel and J. K. Thomas in "Modern Fluorescence Spectroscopy", Vol. 2, E. L. Wehry, Ed., Plenum Press, New York, 1976, p 196.
(13) S. C. Wallace, M. Grätzel, and J. K. Thomas, *Chem. Phys. Lett.*, **23**, 359 (1973).
(14) M. Grätzel and J. K. Thomas, *J. Phys. Chem.*, **78**, 2248 (1974).
(15) S. A. Alkaitis, G. Beck, and M. Grätzel, *J. Am. Chem. Soc.*, **97**, 5723 (1975).
(16) S. A. Alkaitis, M. Grätzel, and A. Henglein, *Ber. Bunsenges. Phys. Chem.*, **79**, 541 (1975).
(17) S. A. Alkaitis and M. Grätzel, *J. Am. Chem. Soc.*, **98**, 3549 (1976).
(18) J. K. Thomas and P. Piciulo, *J. Am. Chem. Soc.*, **100**, 3239 (1978).
(19) Y. Moroi, A. M. Braun, and M. Grätzel, *J. Am. Chem. Soc.*, **101**, 567 (1979).
(20) Y. Moroi, P. P. Infelta, and M. Grätzel, *J. Am. Chem. Soc.*, **101**, 573 (1979).
(21) M. Mangel, *Biochim. Biophys. Acta*, **430**, 459 (1976).
(22) Y. Toyoshima, M. Morino, H. Motoki, and M. Sukigara, *Nature (London)*, **265**, 187 (1977).
(23) W. Stillwell and H. T. Tien, *Biochim. Biophys. Acta*, **81**, 212 (1978).
(24) W. E. Ford, J. W. Ötvös, and M. Calvin, *Nature (London)*, **274**, 507 (1978); *Proc. Natl. Acad. Sci. U.S.A.*, **76**, 3590 (1979).
(25) J. H. Fendler and E. J. Fendler, "Catalysis in Micellar and Macromolecular Systems", Academic Press, New York, 1975.
(26) K. Tamaki, F. Kumamuru, and T. Takayanagi, *Chem. Lett.*, **387** (1977).
(27) T. Kunitake and Y. Okahata, *J. Am. Chem. Soc.*, **99**, 3860 (1977).
(28) K. Deguchi and J. Mino, *J. Colloid Interface Sci.*, **65**, 155 (1978).
(29) C. D. Tran, P. L. Klahn, A. Romero, and J. H. Fendler, *J. Am. Chem. Soc.*, **100**, 1622 (1978).
(30) R. A. Mortara, F. H. Quina, and H. Chaimovich, *Biochim. Biophys. Acta*, **81**, 1080 (1978).
(31) Y. Y. Lim and J. H. Fendler, *J. Am. Chem. Soc.*, **101**, 4023 (1979).
(32) K. Kano, A. Romero, B. Djermouni, H. Ache, and J. H. Fendler, *J. Am. Chem. Soc.*, **101**, 4030 (1979).
(33) A. D. Bangham, *Prog. Biophys. Mol. Biol.*, **18**, 29 (1968).
(34) A. D. Bangham in "Liposomes in Biological Systems," G. Gregoriadis and A. C. Allison, Eds., Wiley, New York, 1979.
(35) J. R. Escabi-Perez, A. Romero, S. Lukac, and J. H. Fendler, *J. Am. Chem. Soc.*, **101**, 2231 (1979).
(36) G. Rothenberger, P. P. Infelta, and M. Grätzel, *J. Phys. Chem.*, **83**, 1871 (1979).
(37) U. Lachish, P. P. Infelta, and M. Grätzel, *Chem. Phys. Lett.*, **62**, 317 (1979).
(38) Typically, 3–15 μL of 1.0 or 4.0 M aqueous sodium chloride solutions were injected into 3.0-mL solutions of $RuC_{18}(bpy)_3^{2+}$ (or $RuC_{18}(bpy)_3^{2+}$ + MPTH, or $RuC_{18}(bpy)_3^{2+}$ + DPTH) in DODAC vesicles. Pulsing was carried out immediately after taking the steady-state absorption and emission spectra.
(39) M. Maestri and M. Grätzel, *Ber. Bunsenges. Phys. Chem.*, **81**, 504 (1977).
(40) For the sake of convenience, the transient absorbance at 510 nm hereafter will be referred to as being due to $MPTH^{+\cdot}$. It has to be borne in mind that it is a composite absorbance, being due to $MPTH^{+\cdot}$ and $RuC_{18}(bpy)_3^{+\cdot}$ (see text). The present results lead us to believe that the decay of the transient at 510 nm is predominantly due to reaction 4 rather than to the separate disappearances of $MPTH^{+\cdot}$ and $RuC_{18}(bpy)_3^{+\cdot}$.
(41) The term "geminate" is used to describe back-reactions of an $MPTH^{+\cdot}$ molecule with its original partner at the very site of its generation. Geminate recombination (reaction 4) was inferred, but its rate was not, of course, observed.